Solid-State NMR Analysis of a Peptide $(Gly\text{-}Pro\text{-}Gly\text{-}Gly\text{-}Ala)_6\text{-}Gly$ Derived from a Flagelliform Silk Sequence of *Nephila clavipes*

Kosuke Ohgo,[†] Taiji Kawase,[†] Jun Ashida,[‡] and Tetsuo Asakura*,[†]

Department of Biotechnology, Tokyo University of Agriculture and Technology, Koganei, Tokyo 184-8588, Japan, and Varian Technologies Japan Ltd., Minato, Tokyo 108-0023, Japan

Received January 18, 2006; Revised Manuscript Received February 19, 2006

Solid-state NMR is especially useful when the structures of peptides and proteins should be analyzed by taking into account the structural distribution, that is, the distribution of the torsion angle of the individual residue. In this study, two-dimensional spin-diffusion solid-state NMR spectra of ^{13}C-double-labeled model peptides $(GPGGA)_6G$ of flagelliform silk were observed for studying the local structure in the solid state. The spin-diffusion NMR spectra calculated by assuming the torsion angles of the β-spiral structure exclusively could not reproduce the observed spectra. In contrast, the spectra calculated by taking into account the statistical distribution of the torsion angles of the individual central residues in the sequences Ala-Gly-Pro, Gly-Pro-Gly, Pro-Gly-Gly, Gly-Gly-Ala, and Gly-Ala-Gly from PDB data could reproduce the observed spectra well. This indicates that the statistical distribution of the torsion angles should be considered for the structural model of $(GPGGA)_6G$ similar to the case of the model peptide of elastin.

Introduction

Orb-web spinning spiders have as many as seven highly specialized glands, each producing silk with different mechanical properties and functions.[1] Dragline silk fiber, which is the product of the major ampullate gland, has been the most extensively investigated silk fiber because of an interesting combination of high tensile strength, extensibility, and an energy-dissipative viscoelastic response. On the other hand, the study of capture silk fibers of the capture spiral has been limited, although the capture silk fibers provide an interesting contrast in material properties with those of dragline silk fibers. The capture silk has a tensile strength of 0.5 GPa,[2] and it is extremely elastic. It stretches as much as 500−1000%,[3,4] although the toughness is nearly the same for both types of silk fibers.

A motif of amino acid sequence, GPGGX (X is occupied by a limited subset of amino acids: Ala, Ser, Tyr, and Val), is repeated frequently in MaSp2 dragline silk protein and flagelliform silk (core fiber of capture silk) from the golden orb weaver *Nephila clavipes*.[5] This appears as tandem repeats in contiguous sequence fragments that contained as many as 63 consecutive repeats in flagelliform silk and seems to be required for elastomeric behavior of the capture spiral.[5] Similar sequences appear also in other elastomeric proteins, that is, elastin $(VPGVG)$[6−8] and glutenin $(PGQGQQ)$.[9] Their primary repeats have been suggested to form type II β-turns from structural analysis of the Pro-Gly part in an elastin mimetic polypeptide[10−12] and subunit of wheat gluten.[13]

Urry and co-workers built a model structure of an elastin-like peptide, $(VPGVG)_n$, as a continuous coil of type II β-turns interconnected by glycine residues.[10] Repetition of this β-turn gives rise to a right-handed helix termed a "β-spiral". They suggested that the elastomeric restoring force originates from the reduction of librational entropy in the peptide segments linking the β-turns as the elastin coil is stretched, which they coined the "librational elasticity mechanism".[6] The pentapeptide repeat, GPGGX, has been suggested to conform to a β-spiral that is similar to the β-spiral of elastin from the similarity of both sequences, (VPGVG) and (GPGGX).[5, 14]

Solid-state NMR spectroscopy is a powerful tool for determining the structures of peptides and proteins in the solid state, especially for the structural determination of amorphous or semicrystalline samples when X-ray diffraction methods cannot be applied to the structure determination.[15] Thus, solid-state NMR is especially useful when the structure should be analyzed by taking into account the structural distribution, that is, the distribution of the torsion angle of an individual residue.[16−18]

In our previous papers,[17,19] the structure of the elastin mimetic peptide $(VPGVG)_6$ was investigated using solid-state NMR, 2D spin-diffusion NMR, and REDOR (rotational echo double resonance) experiments. Additional structural constraints were provided by ^{13}C isotropic chemical shifts and PDB data of the individual residues in the peptide. The latter information was useful in identifying likely combinations of torsion angles, as the NMR data alone were often not enough to provide a single set of the torsion angles. In essence, this approach drew upon several sets of data to formulate the resulting model, namely, that there is a distribution of conformations in this polypeptide. Other evidence of conformational distribution in elastin mimetic peptides has been reported previously. The vibrational analysis of poly(VPGVG) in the solid state suggested an amorphous phase with a dense net of hydrogen bonds.[20] Molecular dynamics simulations of $(VPGVG)_{18}$ with water molecules indicated that hydrophobic collapse was observed if the starting structure used is an idealized β-spiral. Yao and Hong[18] obtained a bimodal structure distribution for the PG residues in $(VPGVG)_3$ with solid-state NMR. Overall, neither study supports a 100% β-spiral structure in the solid state.

In this paper, the local structure of the repeated GPGGX motifs in flagelliform silk is studied with ^{13}C selectively isotope-

* Corresponding author. Phone & Fax: (+81)-423-83-7733. E-mail: asakura@cc.tuat.ac.jp.

[†] Tokyo University of Agriculture and Technology.

[‡] Varian Technologies Japan Ltd.

10.1021/bm0600522 CCC: $33.50
Published on Web 03/21/2006

Table 1. ^{13}C-Double-Labeled Peptides Synthesized for a 2D Spin-Diffusion NMR Experiment

peptide	information
1. $(GPGGA)_2GPGG[1\text{-}^{13}C]A^{15}[1\text{-}^{13}C]G^{16}PGGA\text{-}(GPGGA)_2G$	$Gly^{16}(\phi,\psi)$
2. $(GPGGA)_3[1\text{-}^{13}C]G^{16}[1\text{-}^{13}C]P^{17}GGA(GPGG)_2G$	$Pro^{17}(\phi,\psi)$
3. $(GPGGA)_3G[1\text{-}^{13}C]P^{17}[1\text{-}^{13}C]G^{18}GA(GPGG)_2G$	$Gly^{19}(\phi,\psi)$
4. $(GPGGA)_3GP[1\text{-}^{13}C]G^{18}[1\text{-}^{13}C]G^{19}A(GPGGA)_2G$	$Gly^{19}(\phi,\psi)$
5. $(GPGGA)_3GPG[1\text{-}^{13}C]G^{19}[1\text{-}^{13}C]A^{20}(GPGGA)_2G$	$Ala^{20}(\phi,\psi)$

labeled corresponding peptides, $(GPGGA)_6G$. The 2D spin-diffusion NMR was observed under off-magic-angle spinning conditions to examine the validity of the β-spiral structure which has been considered as the structure of the sequence. For a comparison, the corresponding NMR spectra were calculated by assuming the statistical distribution of the torsion angles of the individual central residues in the sequences, Ala-Gly-Pro, Gly-Pro-Gly, Pro-Gly-Gly, Gly-Gly-Ala, and Gly-Ala-Gly, selected from PDB data.

Experimental Methods

Materials. We prepared the flagelliform silk model peptide $(GPGGA)_6G$ and its isotopically labeled peptides by solid-phase Fmoc chemistry[21] on a fully automated Pioneer Peptide Synthesis System (Applied Biosystems Ltd., Warrington, UK). The labeled sites of the peptides were summarized in Table 1. Fmoc amino acids, the resin, *O*-(7-azabenzotriazole-1-yl)-*N*,*N*,*N*′,*N*′-tetramethyluronium hexafluorophosphate (HATU), and *N*,*N*-diisopropylethylamine (DIEA) were procured from Applied Biosystems. The solvents of high-purity grade and other chemicals were available locally from Wako Pure Chemical Industries Ltd., Osaka, Japan. Typically, the peptide was assembled on a Fmoc-Gly-PEG-PS resin. The coupling of Fmoc amino acids was performed by HATU. After synthesis, the free peptides were released from the resin by treatment with a mixture of trifluoroacetic acid (TFA), phenol, triisopropylsilane, and water (88:5:2:5 vol %) for 2 h at room temperature. The crude peptide was precipitated with dry diethyl ether and washed repeatedly with cold ether. The precipitate, collected by centrifugation, was dried in vacuo. Then the crude peptides from the TFA-cleavage were purified by HPLC using acetonitrile as an elutant. After purification, acetonitrile was removed by evaporation at 42 °C, and then the aqueous solution of the peptide was lyophilized for 24 h. ^{13}C-labeled amino acids, L-[1-^{13}C]Ala, [1-^{13}C]Gly, and L-[1-^{13}C]Pro, 99% enrichment for each amino acid (Cambridge Isotope Laboratories, Inc. MA), were purchased.

^{13}C CP/MAS NMR. The ^{13}C CP/MAS NMR measurements were conducted on a Chemagnetics CMX-400 spectrometer operating at 100 MHz for the ^{13}C nucleus. A 10-kHz spinning speed and 4-mm rotor size were used. CP was employed for sensitivity enhancement with high-power ^{1}H decoupling during the signal acquisition interval.[22] A ^{1}H 90° pulse width of 3.5-μs duration was used with a 1-ms contact time and a 3-s repetition time. Approximately 16K FIDs were added to generate the spectra. The chemical shifts were represented in parts per million with respect to the external reference adamantane. To make a direct comparison with previous data,[19,23,24] we added 28.8 ppm to the observed chemical shifts to account for TMS. About 40 mg was used for the ^{13}C CP/MAS NMR experiment.

2D OMAS Spin-Diffusion NMR. The 2D off-magic-angle spinning spin-diffusion NMR[25] spectra were obtained with a Varian MERCURYplus 400 NMR spectrometer operating at a magnetic field of 9.4 T, corresponding to a resonance frequency of 100.7 MHz for ^{13}C. A 7-mm Jakobsen-type double-tuned MAS probe was used. Off-magic-angle spinning (OMAS) conditions were $\theta = (\theta_m - 7°)$ (where θ_m represents the magic angle) and sample spinning of 6 kHz (±5 Hz). The angle θ between the static magnetic field and sample spinning axes was determined by the measurements of scaled ^{13}C chemical shielding anisotropy (CSA) spectra of β-quinol methanol under OMAS. The CSA of the benzene carbon of β-quinol methanol is 176 ppm, and therefore the scaling factor and the angle θ were easily calculated from the scaled CSA powder pattern under OMAS. The principal values of the chemical shift tensors for the carbonyl carbon atoms were obtained by 1D slow MAS NMR experiments. The principal values of Ala and Gly residues which are similar to the previous values[26] are obtained. The scaling factor of the 2D spin-diffusion spectra was $^1/_2(3\cos^2\theta - 1) = +0.2$. The mixing time of two seconds was optimized for intramolecular spin-diffusion between enriched carbons in two adjacent residues, such that ~100% of the ^{13}C−^{13}C spin pairs are selected. The contact time was set to 2 ms, and the variable-amplitude CP (VACP) technique was used.[27] All NMR experiments were conducted at room temperature. About 150 mg was used for the spin-diffusion NMR experiment.

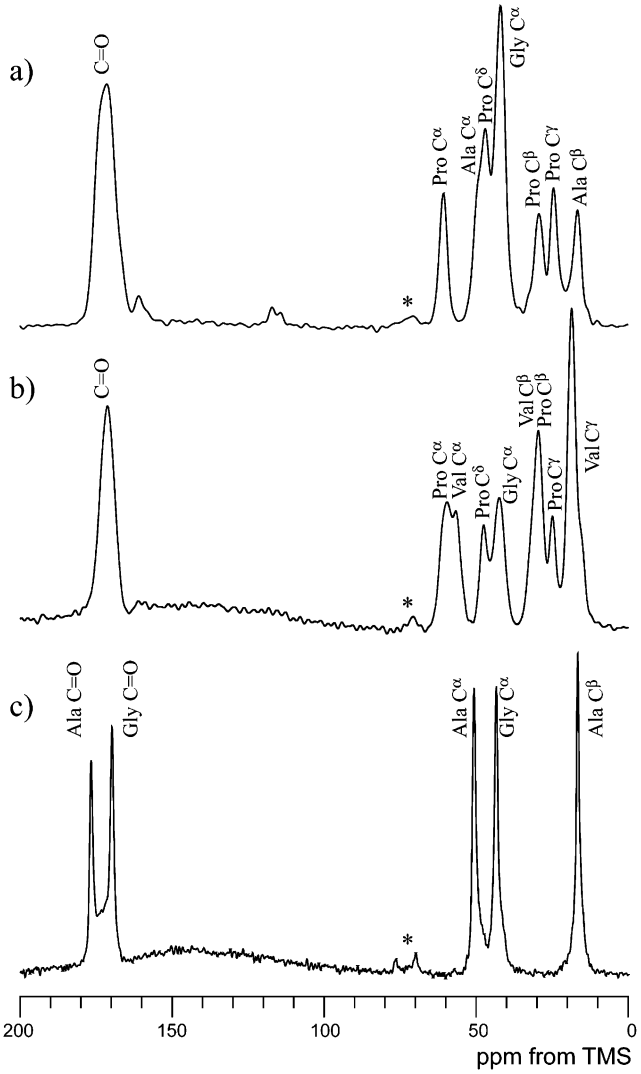

Figure 1. ^{13}C CP/MAS NMR spectra of natural abundance (a) $(GPGGA)_6G$, (b) $(VPGVG)_6$,[17,19] and (c) $(AG)_{15}$ samples.[24,25] No line broadenings were applied in processing these spectra. Spinning sidebands are indicated by asterisks.

Analysis of a 2D Spin-Diffusion NMR Spectrum. A calculation program developed in our laboratory was used to simulate the 2D spin-diffusion NMR spectra.[25] An OCTANE (Silicon Graphics Inc.) workstation was used for the calculation of the theoretical spectra. For simulation of 2D spin-diffusion NMR spectra, the calculations were performed using a grid of 15° for the torsion angles, ϕ and ψ values. To avoid the influence of a strong diagonal peak, the diagonal peaks were neglected in the best-fit analysis.

PDB Analysis. X-ray crystallographic data from the Protein Data Bank[28,29] at the Research Collaboratory for Structural Bioinformatics (RCSB) (http://www.rcsb.org/pdb/) were used to search the torsion

Table 2. Assignment of the ^{13}C CP/MAS NMR Spectrum of $(GPGGA)_6G$ along with the Chemical Shift and Line Width of Each Peak[a]

peptide	peak	chemical shift (ppm)	line width (Hz)
$(GPGGA)_6G$	Ala C^{β}	16.6	243
	Pro C^{γ}	24.3	307
	Pro C^{β}	29.4	293
	Gly C^{α}	41.7	340
	Pro C^{δ}	46.4	268
	Ala C^{α}	49.0	395
	Pro C^{α}	60.7	303
$(AG)_{15}$[b]	Ala C^{β}	16.5	107
	Gly C^{α}	43.2	138
	Ala C^{α}	50.7	131

[a] The corresponding values are also shown for the ^{13}C CP/MAS NMR spectrum of $(AG)_{15}$ for a comparison. [b] Experimental results reported previously.[24,25]

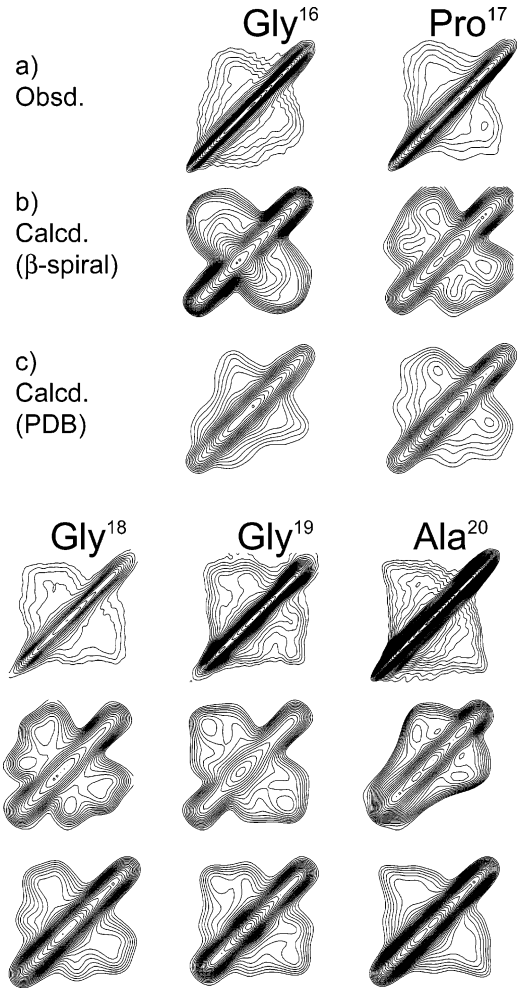

Figure 2. (a) The observed 2D spin-diffusion NMR spectra of the peptides listed in Table 1. A total of 150 t_1 experiments with 178 scans each were recorded, amounting to a total indirect evolution time of 4.9 ms. A ^1H decoupling RF field strength of 76 kHz was used for evolution and acquisition periods. A spectral width was 42 kHz and the ^1H 90° pulse length was 4.3 μs. Line broadening was 100 Hz of Gaussian function. The 2D spin-diffusion spectra calculated (b) by assuming β-spiral and (c) by taking into account the PDB distributions for tripeptide sequences are also shown in Figure 4.

angles of the central residues in the sequences Ala-Gly-Pro, Gly-Pro-Gly, Pro-Gly-Gly, Gly-Gly-Ala, and Gly-Ala-Gly in natural protein. The structures determined at an *R*-factor $\leq$ 20% were used. A subset

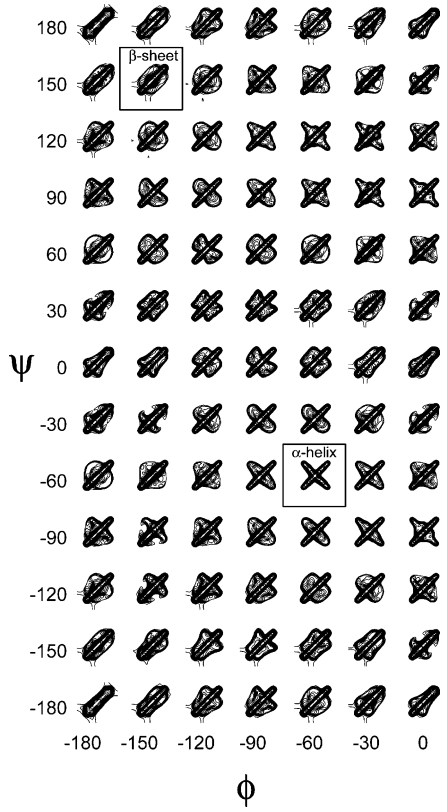

Figure 3. The 2D spin-diffusion NMR spectra calculated for Gly-16 residue as a function of (ϕ, ψ) using increments of 30°. Typical 2D spectral patterns of β-sheet and α-helix are indicated by squares.

of 333 Ala-Gly-Pro, 261 Gly-Pro-Gly, 281 Pro-Gly-Gly, 549 Gly-Gly-Ala, and 582 Gly-Ala-Gly occurrences were obtained from the database after excluding multiple entries of proteins with a similarity greater than 50%. For each pair, the torsion angles of both residues were calculated from the atomic coordinate and were plotted on a Ramachandran map.

Results and Discussion

^{13}C CP/MAS NMR Spectrum of Natural Abundance Peptide, $(GPGGA)_6G$. Figure 1a shows a ^{13}C CP/MAS NMR spectrum of natural abundance $(GPGGA)_6G$ after lyophilization together with the assignment. The ^{13}C CP/MAS NMR spectra of an elastin-mimetic model peptide, $(VPGVG)_6$,[19] and a model peptide of the crystalline domain of *Bombyx mori* silk fibroin, $(AG)_{15}$, in silk I (the structure of *B. mori* silk fibroin before spinning) form reported previously,[24,25] are also shown for comparison (Figure 1, parts b and c, respectively). It is noted that the ^{13}C peaks in the spectra of two elastic peptides $(GPGGA)_6G$ and $(VPGVG)_6$ are significantly broader than those of $(AG)_{15}$; the line widths are larger more than two times as listed in Table 2. In general, the line width of a ^{13}C peak becomes broader with an increase in the structural heterogeneity.[30,31] Actually, the line width of each peak is narrow in the spectrum of $(AG)_{15}$ in silk I form with unique structure (repeated type II β-turn structure) (Figure 1c). In contrast, the structure of $(VPGVG)_6$ has been proposed with the conformational heterogeneity as described in Introduction, and the line width is broad in this case (Figure 1b). Thus, it is expected that $(GPGGA)_6G$ takes the distribution of the local structure, that is, distribution of the torsion angles of each residue rather than interconversion between the conformational state which occurs in solution.[17−19] The ^{13}C chemical shifts of each carbon of

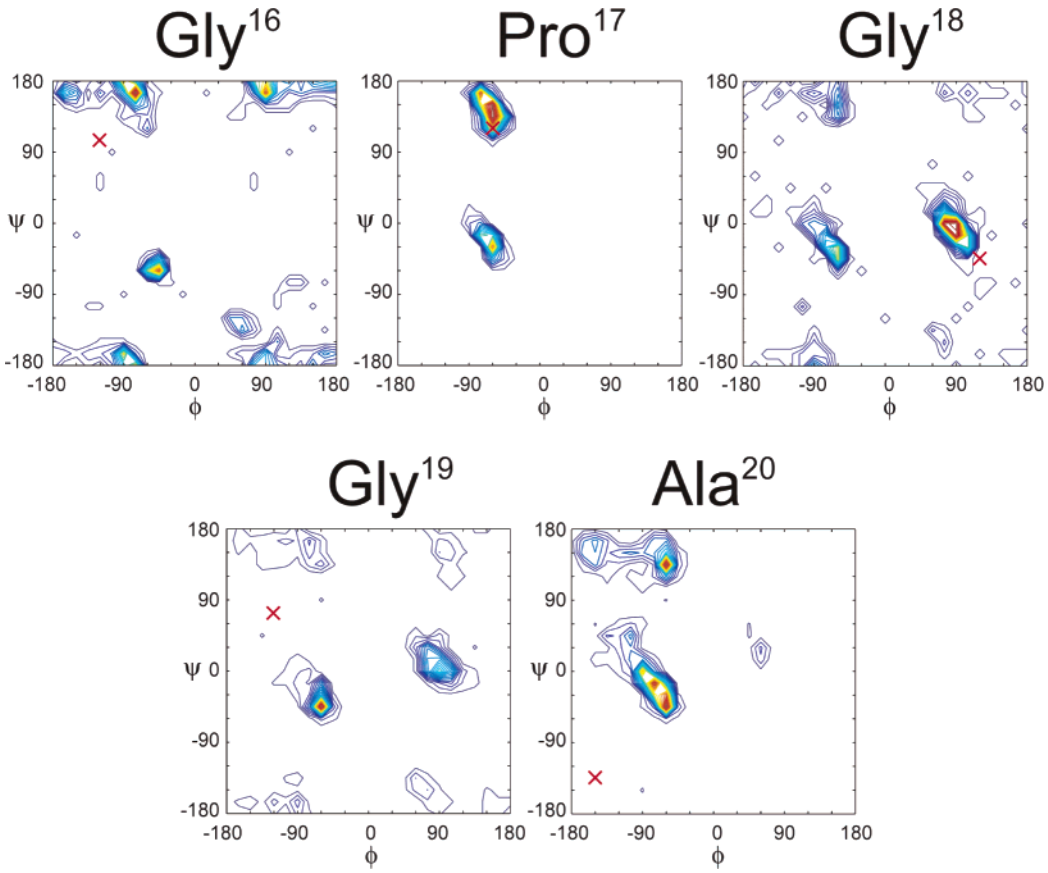

Figure 4. Ramachandran plots of the torsion angles of the individual residues in $(GPGGA)_6G$ by assuming the statistical distribution of the backbone torsion angles of the central residues in the sequences, Ala-Gly-Pro, Gly-Pro-Gly, Pro-Gly-Gly, Gly-Gly-Ala, and Gly-Ala-Gly from PDB. X in the figures indicates the torsion angle of elastin by assuming the β-spiral structure reported previously.[10]

$(GPGGA)_6G$ listed in Table 2 are in agreement with the random coil shifts within experimental error. This indicates that the local structure of the peptide is essentially in random coil.

2D Spin-Diffusion NMR Spectra of the ^{13}C-Double-Labeled Model Peptides, $(GPGGA)_6G$. The observed ^{13}C 2D spin-diffusion NMR spectra of the ^{13}C-double-labeled model peptides, $(GPGGA)_6G$, are shown in Figure 2, together with the calculated spectra by assuming torsion angles of individual residues of the peptide with β-spiral structure[10] or by assuming the statistical distribution of the backbone torsion angles of the central residues in the sequences Ala-Gly-Pro, Gly-Pro-Gly, Pro-Gly-Gly, Gly-Gly-Ala, and Gly-Ala-Gly from PDB. All of the observed spectra of ^{13}C-double-labeled carbonyl carbons of the individual residues of the peptides 1−5 show the patterns with spread of nondiagonal element (Figure 2a). It is noted that the observed patterns are quite different from either β-sheet or α-helix, indicating none of the residues in the peptide take either β-sheet or α-helix (Figure 3) pattern. At first, the structural model "β-spiral" is examined. The torsion angles of β-spiral of elastin, reported previously,[10] are $Gly^{16}(\phi, \psi) = (-120°, 105°)$, $Pro^{17}(\phi, \psi) = (-60°, 120°)$, $Gly^{18}(\phi, \psi) = (120°, -40°)$, $Gly^{19}(\phi, \psi) = (-120°, 80°)$, and $Ala^{20}(\phi, \psi) = (-153°, -132°)$. These torsion angles of the individual residues are used for the calculation of the ^{13}C 2D spin-diffusion NMR spectra. As shown in Figure 2b, the agreement between the calculated and observed spectra was very poor, indicating that the peptide does not take 100% β-spiral structure.

Urry et al. proposed that the repeated pentapeptide sequence, $(VPGVG)_n$, is an essential repeated sequence for producing the elastic character of elastin.[6,7] By employing the mathematical methods of deriving a linear helical correlation structure from a conformation of *cyclo*-$(Val^1\text{-}Pro^2\text{-}Gly^3\text{-}Val^4\text{-}Gly^5)_3$ obtained by X-ray diffraction analysis,[10,11] Urry's group reported the torsion angles as $Val^1(\phi,\psi) = (-120°, 100°)$, $Val^4(\phi,\psi) = (-120°, 80°)$, and $Gly^5(\phi,\psi) = (-150°, -130°)$ together with the Pro-Gly unit ($Pro^2(\phi,\psi) = (-60°, 120°)$ and $Gly^3(\phi,\psi) = (120°, -40°)$). However, in general, cyclo-peptides take limited conformations because of the presence of many constraints such as steric constraints and hydrogen bonding formation as well as "cyclic" without the end groups. The extension of the information on the structures of cyclo-peptides to linear peptides with similar sequence should be performed very carefully. This discussion has already been done in the elastin papers.[19]

Calculation of the2D Spin-Diffusion NMR Spectra of the ^{13}C-Double Labeled Model Peptides, $(GPGGA)_6G$, with Ramachandran Plots of the Torsion Angles Prepared from PDB Data.

Instead of the torsion angles of the β-spiral structure, Ramachandran plots[32] of the torsion angles of the central residues in the sequences Ala-Gly-Pro, Gly-Pro-Gly, Pro-Gly-Gly, Gly-Gly-Ala, and Gly-Ala-Gly in natural protein were used for the calculation of the 2D spin-diffusion NMR spectra. A subset of 333 Ala-Gly-Pro, 261 Gly-Pro-Gly, 281 Pro-Gly-Gly, 549 Gly-Gly-Ala, and 582 Gly-Ala-Gly occurrences were obtained from the database after excluding multiple entries of proteins with a similarity greater than 50%. Figure 4 shows Ramachandran plots of the torsion angles of the individual residues in $(GPGGA)_6G$. Except for the Ramachandran plot of the Gly residue in the sequence Ala-Gly-Pro, two maximum regions tend to appear in the individual Ramachandran plot. By using these plots, the 2D spin-diffusion NMR spectra were calculated and compared with the observed spectra as shown

Table 3. Ranges of the Torsion Angles and Relative Intensities for Each ^{13}C-Labeled Residue of ^{13}C-Labeled $(GPGGA)_6G$ Obtained in This Experiment

residue	torsion angles	relative intensity (%)
Gly-16	$-120° < \phi < -30°$ & $105° < \psi < 180°$	20
	$-75° < \phi < -30°$ & $-75° < \psi < -30°$	10
	β-sheet region	65
Pro-17	$-105° < \phi < -30°$ & $-75° < \psi < 30°$	35
	$-105° < \phi < -30°$ & $90° < \psi < 180°$	65
Gly-18	$45° < \phi < 120°$ & $-45° < \psi < 45°$	40
	$-120° < \phi < -30°$ & $-75° < \psi < 30°$	20
	β-sheet region	30
Gly-19	$45° < \phi < 120°$ & $-45° < \psi < 60°$	30
	$-120° < \phi < -30°$ & $-75° < \psi < 30°$	25
	β-sheet region	35
Ala-20	$-105° < \phi < -30°$ & $-75° < \psi < 15°$	40
	$-90° < \phi < -30°$ & $105° < \psi < 180°$	25
	$-180° < \phi < -120°$ & $120° < \psi < 180°$	15

in Figure 2c. Good agreement was obtained between calculated and observed spectra. This indicates that the 100% β-spiral structural model is invalid as the structural model of $(GPGGA)_6G$. Instead of this, the distribution of the torsion angles should be considered as the structure of the peptide. The distribution of the torsion angles is summarized in Table 3 for the individual residues of $(GPGGA)_6$.

This study clearly shows that the seemingly simple pentapeptide subunit does not adopt a single, well-defined conformation (Table 3). We attempt to describe the local structure of the -Pro-Gly- sequence by focusing on the torsion angles corresponding to the major component in the conformational distribution of each residue as follows. The set of the torsion angles is $-105° < \phi < -30°$ and $90° < \psi < 180°$ for Pro,[17] and it is $45° < \phi < 120°$ and $-45° < \psi < 45°$ for Gly.[18] To reconcile the torsion angles corresponding to the major component of the conformational distributions, a type II β-turn structure was assigned to about 40% of the Pro-Gly pair. The other set, $-105° < \phi < -30°$ and $-75° < \psi < 30°$ for Pro[17] and $-120° < \phi < -30°$ and $-75° < \psi < 30°$ for Gly,[18] implies a type I β-turn structure assigned to about 20%. Zhou et al. synthesized a flagelliform silk analogue protein $[(GPGGSGPGGY)_2GPGGK]_n$ by using recombinant DNA techniques and analyzed the structure of this protein in aqueous solution and in the solid state.[33] NMR investigations of the secondary structure of this protein indicated the presence of type II β-turns among the conformational population in aqueous solutions, and CD analysis indicated approximately 20% turn content in aqueous solution. Moreover, the solid-state CD and FTIR data indicated an increase in the β-turn population compared with aqueous solution and suggested the conformational mixture of β-turn conformations of type I and type II and the presence of random-coil or open conformers. These data are consistent with our assignment of the local structure of the Pro-Gly sequence.

Acknowledgment. T.A. acknowledges support from the Insect Technology Project, Japan, and the Agriculture Biotechnology Project, Japan.

References and Notes

(1) Vollrath, F. *Sci. Am.* **1992**, *266*, 70−76.
(2) Gosline, M. J.; Guerette, A. P.; Ortlepp, S. C.; Savage, N. K. *J. Exp. Biol.* **1999**, *202*, 3295−3303.
(3) Opell, B. D.; Bond, J. E. *Biol. J. Linnean Soc.* **2000**, *70*, 107−120.
(4) Vollrath, F.; Edomonds, D. T. *Nature* **1989**, *340*, 305−307.
(5) Hayashi, C. Y.; Lewis, R. V. *J. Mol. Biol.* **1998**, *275*, 773−784.
(6) Urry, D. W. *J. Protein Chem.* **1988**, *7*, 1−34.
(7) Urry, D. W. *J. Protein Chem.* **1988**, *7*, 81−114.
(8) Urry, D. W. *J. Phys. Chem. B* **1997**, *101*, 11007−11028.
(9) Shewry, P. R.; Halford, N. G.; Tatham, A. S. *J. Cereal Sci.* **1992**, *15*, 105−120.
(10) Venkatachalam, C. M.; Urry, D. W. *Macromolecules* **1981**, *14*, 1225−1229.
(11) Cook, W. J.; Einspahr, H.; Trapane, T. L.; Urry, D. W.; Bugg, C. E. *J. Am. Chem. Soc.* **1980**, *102*, 5502−5505.
(12) Urry, D. W.; Chang, D. K.; Krishna, N. R.; Huang, D. H.; Trapane, T. L.; Prasad, K. U. *Biopolymers* **1989**, *28*, 819−833.
(13) Tatham, A. S.; Drake, A. F.; Shewry, P. R. *J. Cereal Sci.* **1990**, *11*, 189−200.
(14) Hayashi, C. Y.; Shipley, N. H.; Lewis, R. V. *Int. J. Biol. Macromol.* **1999**, *24*, 271−275.
(15) *NMR Spectroscopy of Biological Solids*; Ramamoorthy, A., Ed.; Taylor & Francis, Boca Raton, FL, 2005.
(16) van Beek, J. D.; Beaulieu, L.; Schafer, H.; Demura, M.; Asakura, T.; Meier, B. H. *Nature* **2000**, *405*, 1077−1079.
(17) Asakura, T.; Ashida, J.; Ohgo, K. *Polymer J.* **2003**, *35*, 293−296.
(18) Yao, X. L.; Hong, M. *J. Am. Chem. Soc.* **2004**, *126*, 4199−4210.
(19) Ohgo, K.; Ashida, J.; Kumashiro, K. K.; Asakura, T. *Macromolecules* **2005**, *38*, 6038−6047.
(20) Rodriguez-Cabello, J. C.; Alonso, M.; Diez, M. I.; Caballero, M. I.; Herguedas, M. M. *Macromol. Chem. Phys.* **1999**, *200*, 1831−1838.
(21) Carpino, L. A.; Han, G. Y. *J. Am. Chem. Soc.* **1970**, *92*, 5748−5749.
(22) Pines, A.; Gibby, M. G.; Waugh, J. S. *J. Chem. Phys.* **1973**, *59*, 569−590.
(23) Ashida, J.; Ohgo, K.; Komatsu, K.; Kubota, A.; Asakura, T. *J. Biomol. NMR* **2003**, *25*, 91−103.
(24) Asakura, T.; Ohgo, K.; Komatsu, K.; Kanenari, M.; Okuyama, K. *Macromolecules* **2005**, *38*, 7397−7403.
(25) Asakura, T.; Ashida, J.; Yamane, T.; Kameda, T.; Nakazawa, Y.; Ohgo, K.; Komatsu, K. *J. Mol. Biol.* **2001**, *306*, 291−305.
(26) Wei, Y.; Lee, D. K.; Ramamoorthy, A. *J. Am. Chem. Soc.* **2001**, *123*, 6118−6126.
(27) Peersen, O. B.; Wu, X. L.; Kustanovich, I.; Smith, S. O. *J. Magn. Reson. A* **1993**, *104*, 334−339.
(28) Bernstein, F. C.; Koetzle, T. F.; Williams, G. J. B.; Meyer, E. F., Jr.; Brice, M. D.; Rodgers, J. R.; Kennard, O.; Shimanouchi, T.; Tasumi, M. *J. Mol. Biol.* **1977**, *112*, 535−542.
(29) Berman, H. M.; Westbrook, J.; Feng, Z.; Gilliland, G.; Bhat, T. N.; Weissig, H.; Shindyalov, I. N.; Bourne, P. E. *Nucleic Acids Res.* **2000**, *28*, 235−242.
(30) Martin, R. W.; Zilm, K. W. *J. Magn. Reson.* **2003**, *165*, 162−174.
(31) Balbach, J. J.; Petkova, A. T.; Oyler, N. A.; Antzutkin, O. N.; Gordon, D. J.; Meredith, S. C.; Tycko, R. *Biophys. J.* **2002**, *83*, 1205−1216.
(32) Ramachandran, G. N.; Ramakrishnan, C.; Sasisekharan, V. *J. Mol. Biol.* **1963**, *7*, 95−99.
(33) Zhou, Y.; Wu, S.; Conticello, V. P. *Biomacromolecules* **2001**, *2*, 111−125.

BM0600522